Journal of
Materials Chemistry B

Materials for biology and medicine

Accepted Manuscript

This article can be cited before page numbers have been issued, to do this please use: P. Sharma, A. Venugopal, C. M. Verdi, M. S. Roger, A. Calò and M. Kumar, *J. Mater. Chem. B*, 2024, DOI: 10.1039/D4TB00862F.

ROYAL SOCIETY OF CHEMISTRY

rsc.li/materials-b

View Article Online
DOI: 10.1039/D4TB00862F

COMMUNICATION

Heparin Binding Induced Supramolecular Chirality into Self-Assembly of Perylenediimide bolaamphiphile

Received 00th January 20xx,
Accepted 00th January 20xx

DOI: 10.1039/x0xx00000x

Poonam Sharma,[a,†] Akhil Venugopal,[a,b,†] Claudia Martínez Verdi,[a] Mauri Serra Roger,[a] Annalisa Calò[b,c,d] and Mohit Kumar*[a,b,e]

Chirality is one of the hallmark of biomolecules. Here we utilize heparin, a chiral biomolecule and a potent drug, to induce chiral organization into the assembly of achiral molecule. Polyanionic heparin binds with dicationic perylenediimide derivative to induce supramolecular helical organization in aqueous medium as well as in a highly competitive cell culture medium.

Helical supramolecular polymers, formed by the self-assembly of chiral molecules, have been extensively investigated as a model system to understand homochiral preference in nature and for various chiroptical functionalities.[1-11] More recently, it has been shown that the presence of chiral guest molecules, chiral solvents or other chiral forces can induce supramolecular chirality into the self-assembly of achiral molecules.[12-18] Such chiral guest assisted induction of chirality has resulted in various helical supramolecular polymers for applications in asymmetric catalysis, chiral separation, circularly polarized luminescence, detection of stereoisomeric purity etc.[19-25] However, induction of chirality upon binding with biomolecular chiral guests are less investigated but opens up new avenues for biotechnological applications like sensing and diagnostics.[26-30] In this regard, George and coworkers among others have demonstrated adenosine phosphate binding induced supramolecular helicity for probing biochemical reactions, actin mimetic seeded supramolecular polymerization, chemically fueled transient helical structure etc.[26, 31-35] However, use of heparin, which is a chiral biomolecule and a drug, to induce supramolecular order and helicity into the assembly of functional molecules will be of potential use in diagnostics and therapeutics.

Heparin is a chiral, naturally occurring polysaccharide that is widely used in medicine for its anti-coagulant properties.[36]

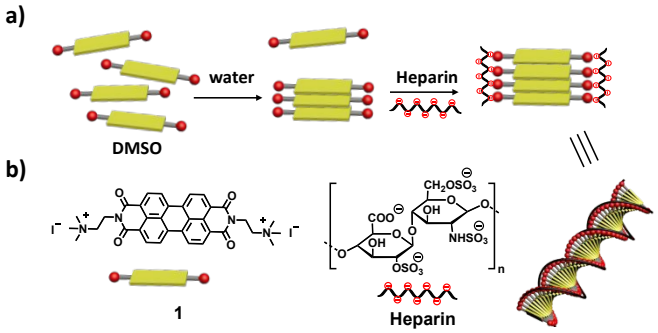

Scheme 1. Schematic representation of a) heparin binding induced chiral self-assembly of **1** and b) molecular structure of **1** and heparin.

Because of its biomedical relevance, heparin responsive molecular and supramolecular systems have been an active area of research. The polyanionic nature of heparin, due to the high degree of sulfation, has been used to bind to positively charged molecules, self-assembled systems, nanoparticles for sensing applications.[37-40] Even though heparin responsive supramolecular polymers are known, heparin binding induced supramolecular chirality is very rarely reported.[41-44] Furthermore, heparin induced chiral organization on well-known arylene diimides derivatives is never reported, and thus will be of significant interest in various chirotechnological applications.

Here we report heparin binding induced supramolecular chirality into the self-assembly of perylene diimide (PDI) derivative **1** (Scheme 1). The molecular design of **1** includes i) a PDI aromatic core which has been shown to self-assemble in water due to π-π interaction and, ii) positively charged trimethylammonium derivative which can electrostatically bind to negatively charged heparin. We demonstrate that the negatively charged, chiral heparin biopolymer binds to the positively charged **1** to facilitate self-assembly and induce supramolecular chirality into the self-assembly of achiral PDI derivative. Previous reports on self-assembly of **1** and similar PDI derivatives have been about demonstrating the role of

[a] Department of Inorganic and Organic Chemistry, University of Barcelona, Calle Marti i Fraquès 1-11, 08028 Barcelona (Spain). Email: mohit.kumar@ub.edu
[b] Institute for Bioengineering of Catalonia (IBEC), Calle Baldiri Reixac 10–12, 08028 Barcelona (Spain)
[c] Department of Electronic and Biomedical Engineering, University of Barcelona, Calle Marti i Fraquès 1-11, 08028 Barcelona (Spain)
[d] Institute of Nanoscience and Nanotechnology, University of Barcelona, 08028 Barcelona (Spain)
[e] Institut de Química Teòrica i Computacional, University of Barcelona, 08028 Barcelona (Spain)
† These authors contributed equally.
Electronic Supplementary Information (ESI) available: Supporting figures and other details are included here. See DOI: 10.1039/x0xx00000x

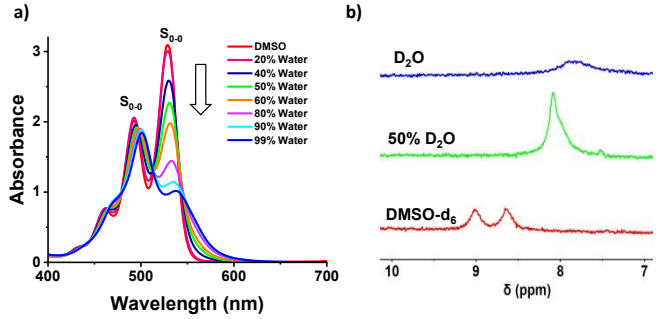

Figure 1. a) UV-Vis absorption spectra of **1** (0.05 mM) in varying % of water in DMSO and b) Partial NMR spectra showing aromatic region of **1** (1 mM) in DMSO-d_6, 50 % D_2O and in D_2O alone.

solvents in self-assembly, charge transfer complexation, protein sensing,[45-47] including adenosine triphosphate responsive chiral assembly.[26, 30] Here, for the first time, we demonstrate heparin binding assisted supramolecular ordering and induction of helicity into self-assembly of **1** in aqueous as well as in biological cell culture medium.

The self-assembly of **1** was investigated in different solvent compositions of DMSO-water by recording both the UV-Vis absorption and emission spectra. The compound **1** was monomeric in DMSO (0.05 mM) as evident from the well-defined vibronic absorption bands with peaks at 492 nm (S_{0-1} band), 530 nm (S_{0-0} band) (Figure 1a). Upon increasing percentage of water, we observe a broadening of these bands with a continuous decrease in absorbance of the 530 nm band without significant change in the 492 nm band. This leads to a change in which the 500 nm peak becomes the absorption maxima in 99% water compared to 530 nm band in DMSO i.e. a 30 nm blue shift.[48] These spectral features indicate the formation of a face-to-face H-aggregate of **1** in water.[45, 49-50] Furthermore, the ratio of absorbance at S_{0-0} to S_{0-1} band (S_{0-0}/S_{0-1}), which is known to be a signature of self-assembly in PDI derivative, decreased from 1.5 in DMSO to 0.7 in 99% water, further confirming the self-assembly of **1** in water.

The fluorescence spectra of **1** in DMSO shows sharp emission bands at 550 nm with a shoulder at 585 nm which is known to originate from the monomeric form of PDI (Figure S1). Upon self-assembly of **1** in increasing percentage of water, we observe that the fluorescence spectral features are similar to the monomeric form which was further validated by the excitation spectra (Figure S1c). Thus, we confirm that the self-assembly of **1** in increasing % of water result in non-fluorescent H-aggregates, and any observed fluorescence arises from the residual monomers. Unexpectedly, we observed an increase in monomeric fluorescence intensity till 40% water followed by fluorescence quenching till 99% water. Similar observation was recently reported by Rao and coworkers and it was assigned to be due to preferential solvation.[45] However, we could not extrapolate this reported explanation in our case as it was not consistent with all of our observations. Thus, we performed

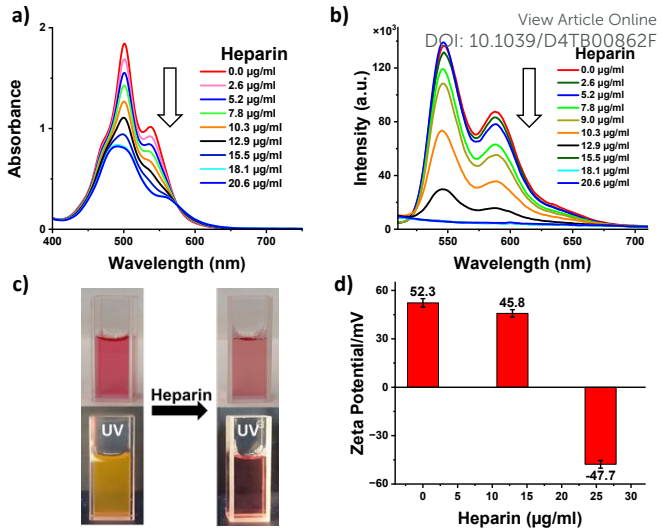

Figure 2. a) Absorption and b) emission spectra of **1** in the presence of different concentrations of heparin; c) Visible (above) and fluorescence (under 365 nm UV light, below) photographs of **1** before and after the addition of heparin; and d) Variation of zeta potential of self-assembled **1** in the presence of different concentrations of heparin in 99% water. Concentration of **1** = 0.05 mM; solvent: 99% water in DMSO, optical path length for absorption spectra= 10mm and for fluorescence spectra= 1mm.

detailed investigation to reveal that the inherent quantum yield of the monomers of **1** is much higher in 40% water (44% quantum yield) compared to DMSO alone (7% quantum yield) as shown in Figure S2. Thus, even though the concentrations of monomers decrease with increasing water ratio, the fluorescence intensity is much higher in 40% water compared to DMSO. Furthermore, the photos of the sample solutions show visible color change in line with the spectroscopic observations, to confirm the formation of self-assembled **1** (Figure S1b). Further analysis with the ^1H NMR spectroscopy shows broadening and upfield shift of the aromatic protons of **1** from 8.85 to 7.84 ppm upon going from DMSO-d_6 to D_2O (Figure 1b). These observations clearly indicate water assisted self-assembly of **1** through π-π interactions of PDI (Scheme **1**).

Having investigated the self-assembly of **1**, we probed the effects of binding with heparin leading to co-assembly of **1** with heparin. Thus, increasing amount of heparin was added to a pre-assembled solution of **1** in 99% water and the changes were monitored with absorption spectroscopy (Figure 2a). We observed a gradual broadening of the peaks along with a decrease in absorbance and the appearance of a new broad band at around 600 nm, with an isosbestic point at 575 nm. These clearly indicate a supramolecular reconfiguration of self-assembly of **1** upon binding with heparin. Furthermore, the S_{0-0}/S_{0-1} band ratios decreased from 0.7 to 0.5 (Figure S3) and the fluorescence measurements showed a continuous quenching of emission (Figure 2b). Additionally, the photos of the sample solutions under ambient condition and under 365 nm light show visible color change and fluorescence quenching, further confirming the co-assembly between heparin and **1** (Figure 2c). These data clearly indicate heparin binding induced enhanced intermolecular interaction of **1** leading to supramolecular

View Article Online
DOI: 10.1039/D4TB00862F

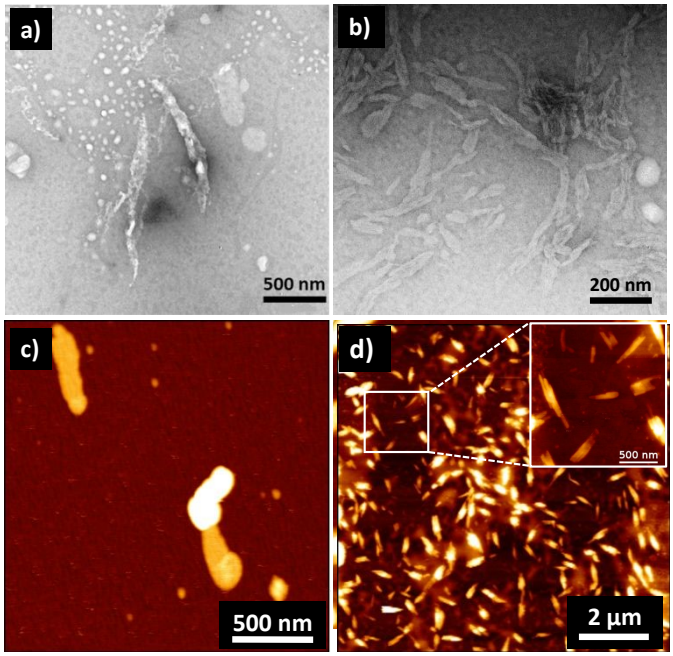

Figure 3. TEM images in the absence a) and presence b) of heparin showing heparin-induced self-assembly of **1**. c) and d) are the corresponding AFM images of samples without and with heparin respectively. Concentration of **1** = 0.05 mM; solvent: 99% water in DMSO, concentration of heparin = 25.8 µg/ml. TEM samples were stained with 2% Uranyl acetate solution. In the literature, self-assembly of **1** in water is shown to form nanofibers in water, but they were reported in 2-10 times higher concentration than our working concentration.[30, 45]

reorganization. To confirm the type of interaction between heparin and **1**, zeta potential measurements were performed. The positive zeta potential of self-assembled **1** (+52.3 mV) decreased substantially and ultimately become negative (-47.7 mV) with the addition of heparin (Figure 2d). The change in zeta potential value clearly confirms that the electrostatic interaction between the positively charged **1** and negatively charged heparin is responsible for the binding. Furthermore, Dynamic light scattering (DLS) experiment also demonstrated a change in size distribution of the self-assembled structure upon binding with heparin, indicating a change in supramolecular order (Figure S8).

Till now, we have shown that heparin successfully binds to both the self-assembled and the monomeric form of **1** which result in spectroscopic changes that indicate supramolecular reorganization. We next used the transmission electron microscopy (TEM) and atomic force microscopy (AFM) techniques to understand the morphological transformation associated with heparin binding. Thus, a sample of **1** in 99% water (with or without heparin) was drop-casted and dried on TEM grid for TEM imaging and the same was done on mica for AFM imaging. TEM micrographs show the formation of self-assembled structures of **1** which are not fully well-defined, but could be bundles of short fibers and they were sparsely populated (Figure 3a, c, S4 and S6). Interestingly, binding of heparin resulted in the formation of well-defined fibers which are visibly abundant in all the micrographs (Figure 3b, d, S5 and S6). We could not observe individual fibers due to the tendency of these nanostructures to form bundles, probably because polymeric heparin can bind to multiple fibers simultaneously. However, AFM height analysis provided insight into the molecular organization within the nanostructure (Figure S7). The thickness of some of the fibers was obtained from the height analysis of the nanostructures using AFM. The thinnest fibers were approximately 4 nm in height. Since the molecular length of **1** is around 2 nm and the width of the heparin chain is of the order of 1 nm, the 4 nm fiber height is consistent with **1** bound by heparin on both sides and the length of fiber is expected to be the direction of π-π interactions, as shown in scheme **1** and scheme **S1**.

After confirming the heparin binding induced supramolecular transformation, we next probed the ability of heparin to induce chiral organization into the assembly of achiral **1**. Thus, the circular dichroism (CD) measurements of **1** in the absence and presence of heparin were performed. Derivative **1** is molecularly achiral and therefore its self-assembly in 99% water do not show any CD signal (Figure 4a and Figure S10), indicating achiral or racemic organization. However, binding of heparin, as the chiral guest molecule, to self-assembled **1** is expected to result in a chiral complex with defined CD signal. We observed that the addition of heparin to a solution of **1** in 99% water resulted in a positive monosignated CD signal with peak maxima at 510 nm (Figure S10a). This does indicate an induction of chirality from heparin to the assembly of **1**, but it lacks the bisignated CD signal obtained for a typical helical organization. Such monosignated CD signal could be due to the asymmetric perturbation of the electronic transitions of **1** by the neighbouring chiral centres in heparin, without producing a helical organization of **1**.[41] This could be because in 99% water, there is stronger intermolecular interactions between the molecules of **1** and thus lack the conformational flexibility to rearrange into a helical organization upon heparin binding.

To confirm the above hypothesis, we performed the heparin binding measurements of **1** in a sample containing a lower percentage of water in which case **1** is expected to be weakly assembled. The addition of heparin to a 50% water in DMSO solution of **1** demonstrated heparin binding induced self-assembly as observed by absorption, fluorescence, and NMR spectroscopic and zeta potential measurements (Figure S3b,d, S11 and S14). Finally, the CD measurements were performed upon the addition of heparin to a 50% water in DMSO solution of **1**. We observed a well-defined negative bisignated CD signal with a negative maximum at 510 nm followed by a positive maximum at 465 nm (Figure 4a). This clearly confirms heparin binding induced excitonic coupling of PDI chromophores of **1**

View Article Online
DOI: 10.1039/D4TB00862F

COMMUNICATION

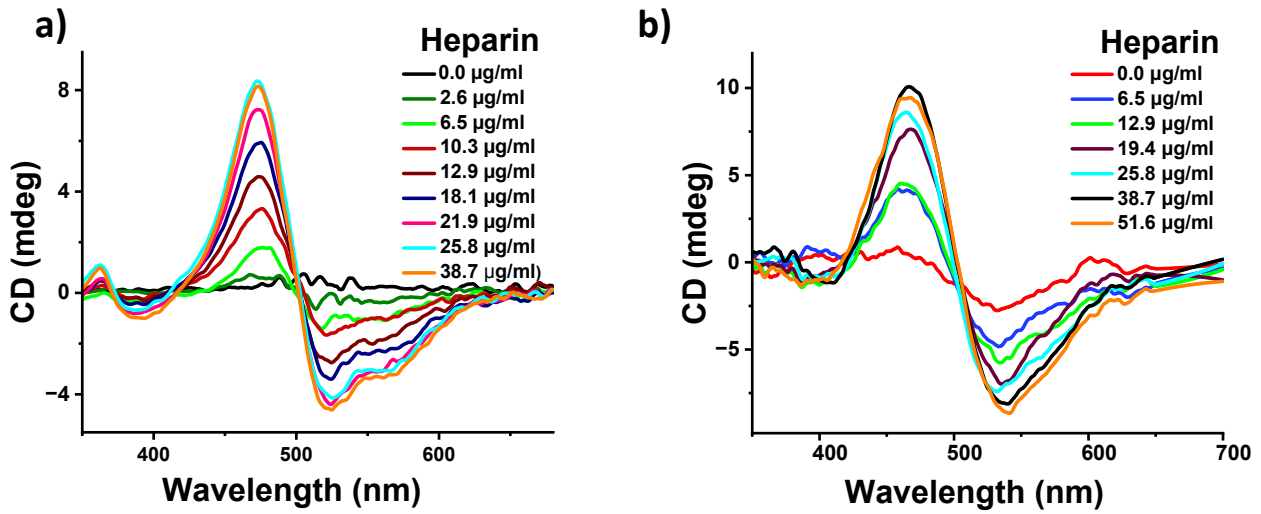

Figure 4 a) Circular dichroism spectrum of derivative **1** in 50% water in the presence of various concentrations of heparin; b) Circular dichroism spectrum of derivative **1** in 50% fetal bovine serum (FBS) in the presence of various concentrations of heparin. The weak CD signal in b) in the absence of heparin can be due to the presence of small amount of heparin in the FBS medium or other protein molecules present in such a complex fluid.

resulting in a left-handed helical assembly. As expected, the value of CD signal increased gradually with the increasing concentration of heparin. This was also followed by morphological transformation from a random aggregate to a 2-dimensional sheet like structure upon addition of heparin to **1** in 50% water sample (Figure S9). Similar bisignated CD signals were also obtained with 20% water in DMSO and pure DMSO sample further confirming that conformational flexibility within the self-assembled structure of **1** is essential for induction of supramolecular helicity upon binding with heparin (Figure S10). It is to be pointed out that even though **1** is monomeric in DMSO, binding to heparin results in aggregation of **1** (Figure S10 e-f) and therefore CD signal originates from the heparin bound self-assembly of **1**. To our knowledge, this is the first example where heparin has been used as a chiral guest to induce supramolecular helicity into the assembly of any arylenediimide derivatives and more specifically perylenediimide derivative. Moreover, heparin binding experiments were also performed in pH 7.4 buffer condition which also showed similar behavior, ruling out any pH change based effects (Figure S12, 13).

Since heparin is a biomolecule which is naturally present in human body and is also used as a drug for therapeutic purposes, we tested if heparin induced supramolecular helicity can also be observed in biologically relevant conditions. Thus, we investigated the applicability of our system in fetal bovine serum (FBS) which mimic human blood samples and cell culture medium. Additionally, heparin binding was investigated in a solvent containing 50% aqueous FBS medium in DMSO. We observed a similar negative bisignated CD signal with increasing signal intensity upon increasing amount of heparin (Figure 4b). These changes were also accompanied by the absorption spectral changes confirming heparin binding induced supramolecular organization of **1** in FBS (Figure S15). It is to be noted that heparin binding is challenging in a biological media like FBS as it is a complex mix of several proteins, enzymes and high concentration of organic and inorganic salts. Our observation of successful heparin binding induced supramolecular changes into the assembly of **1** in such a highly competitive FBS medium clearly indicates the strong affinity and the effect of molecular recognition. Furthermore, the ability of our system to demonstrate heparin induced spectroscopic changes in biological conditions and blood-mimicking media will be most suited for application in sensing and diagnostics.

Conclusions

In summary, we have presented a novel design of heparin binding assisted supramolecular organization and induction of helicity into the self-assembly of achiral perylenediimide chromophores. The cationic achiral PDI derivative binds to anionic chiral heparin biomolecule through electrostatic interactions to result in the formation of chiral 1-dimensional nanostructures. Detailed spectroscopic and microscopic investigations provided insights into the mode of self-assembly

and the mechanism of chirality induction process. Furthermore, the heparin induced supramolecular helicity could also be achieved in a highly competitive, cell culture medium like FBS. Considering the relevance of heparin as an essential biomolecule and a well-known drug, this work will be of potential relevance in biomedicine. Our simple and versatile design of anionic biopolymer responsive assembly will be further studied with other highly relevant biomolecules like Chondroitin-Sulphate.

Author Contributions

MK conceived the idea, CMV and MSR did the synthesis and preliminary spectroscopic studies. PS and AV performed most of the spectroscopic and microscopic investigations. AC did the AFM imaging and analysis. PS and MK wrote the manuscript. All the authors read and commented on the manuscript.

Conflicts of interest

"There are no conflicts to declare".

Acknowledgements

The authors acknowledge funding from Proyectos de Generación de Conocimiento 2021 grant from the Spanish ministry of science and innovation (PID2021-126244NA-I00). MK acknowledges the Ramon y Cajal fellowship from the Spanish ministry of science and innovation. AC acknowledges the Foundation "Bartolo Longo III Millennio", and the Institute of Nanoscience and Nanotechnology of UB (IN^{2}UB) under the project Ajut a la Recerca Transversal (ART 2020) for financial support.

Notes and references

1. V. K. Praveen, S. S. Babu, C. Vijayakumar, R. Varghese and A. Ajayaghosh, *Bull. Chem. Soc. Jpn.*, 2008, **81**, 1196-1211.
2. E. Yashima, N. Ousaka, D. Taura, K. Shimomura, T. Ikai and K. Maeda, *Chem. Rev.*, 2016, **116**, 13752-13990.
3. M. M. Safont-Sempere, V. Stepanenko, M. Lehmann and F. Würthner, *J. Mater. Chem.*, 2011, **21**, 7201-7209.
4. M. Weh, K. Shoyama and F. Würthner, *Nat. Commun.*, 2023, **14**, 243.
5. P. A. Korevaar, S. J. George, A. J. Markvoort, M. M. Smulders, P. A. Hilbers, A. P. Schenning, T. F. De Greef and E. Meijer, *Nature*, 2012, **481**, 492-496.
6. M. Kumar, N. L. Ing, V. Narang, N. K. Wijerathne, A. I. Hochbaum and R. V. Ulijn, *Nat. Chem.*, 2018, **10**, 696-703.
7. M. A. Martínez, A. Doncel-Giménez, J. Cerdá, J. Calbo, R. Rodríguez, J. Aragó, J. Crassous, E. Ortí and L. Sánchez, *J. Am. Chem. Soc.*, 2021, **143**, 13281-13291.
8. F. García, R. Gómez and L. Sánchez, *Chem. Soc. Rev.*, 2023, **52**, 7524-7548.
9. T. Aida, E. W. Meijer and S. I. Stupp, *Science*, 2012, **335**, 813-817.
10. R. Zheng, M. Zhao, J. S. Du, T. R. Sudarshan, Y. Zhou, A. K. Paravastu, J. J. De Yoreo, A. L. Ferguson and C. L. Chen, *Nat. Commun.*, 2024, **15**, 3264.
11. R. Sethy, J. Kumar, R. Métivier, M. Louis, K. Nakatani, N. M. T. Mecheri, A. Subhakumari, K. G. Thomas, T. Kawai and T. Nakashima, *Angew. Chem. Int. Ed.*, 2017, **56**, 15053-15057.
12. W. Zhang, W. Jin, T. Fukushima, N. Ishii and T. Aida, *J. Am. Chem. Soc.*, 2013, **135**, 114-117.
13. M. Wolffs, S. J. George, Ž. Tomović, S. C. Meskers, A. P. Schenning and E. e. W. Meijer, *Angew. Chem. Int. Ed.*, 2007, **46**, 8203-8205.
14. S. J. George, R. de Bruijn, Z. e. Tomović, B. Van Averbeke, D. Beljonne, R. Lazzaroni, A. Schenning, PHJ and E. Meijer, *J. Am. Chem. Soc.*, 2012, **134**, 17789-17796.
15. S. Sevim, A. Sorrenti, J. P. Vale, Z. El-Hachemi, S. Pané, A. D. Flouris, T. S. Mayor and J. Puigmartí-Luis, *Nat. Commun.*, 2022, **13**, 1766.
16. A. Sorrenti, R. Rodriguez-Trujillo, D. B. Amabilino and J. Puigmartí-Luis, *J. Am. Chem. Soc.*, 2016, **138**, 6920-6923.
17. N. Petit-Garrido, J. Claret, J. Ignés-Mullol and F. Sagués, *Nat. Commun.*, 2012, **3**, 1001.
18. G. Ouyang, J. Rühe, Y. Zhang, M. J. Lin, M. Liu and F. Würthner, *Angew. Chem. Int. Ed.*, 2022, **134**, e202206706.
19. K. Shimomura, T. Ikai, S. Kanoh, E. Yashima and K. Maeda, *Nat. Chem.*, 2014, **6**, 429-434.
20. K. Fu and G. Liu, *ACS nano*, 2024, **18**, 2279-2289.
21. A. Das, S. Ghosh and S. J. George, *Angew. Chem. Int. Ed.*, 2023, **135**, e202308281.
22. F. Riobé, A. P. Schenning and D. B. Amabilino, *Org. Biomol. Chem.*, 2012, **10**, 9152-9157.
23. J. C. Ng, J. Liu, H. Su, Y. Hong, H. Li, J. W. Lam, K. S. Wong and B. Z. Tang, *J. Mater. Chem. C*, 2014, **2**, 78-83.
24. K. Salikolimi, V. K. Praveen, A. A. Sudhakar, K. Yamada, N. N. Horimoto and Y. Ishida, *Nat. Commun.*, 2020, **11**, 2311.
25. J. Han, J. You, X. Li, P. Duan and M. Liu, *Adv. Mater.*, 2017, **29**, 1606503.
26. T. Ma, C. Li and G. Shi, *Langmuir*, 2008, **24**, 43-48.
27. Z. Li, S. Li, Y. Guo, C. Yuan, X. Yan and K. S. Schanze, *ACS nano*, 2021, **15**, 4979-4988.
28. H. Nian, L. Cheng, L. Wang, H. Zhang, P. Wang, Y. Li and L. Cao, *Angew. Chem. Int. Ed.*, 2021, **133**, 15482-15486.
29. J. Xiao, J. Xu, S. Cui, H. Liu, S. Wang and Y. Li, *Org. Lett.*, 2008, **10**, 645-648.
30. S. K. Sen, R. D. Mukhopadhyay, S. Choi, I. Hwang and K. Kim, *Chem*, 2023, **9**, 624-636.
31. A. Mishra, D. B. Korlepara, M. Kumar, A. Jain, N. Jonnalagadda, K. K. Bejagam, S. Balasubramanian and S. J. George, *Nat. Commun.*, 2018, **9**, 1295.
32. S. Dhiman, A. Jain, M. Kumar and S. J. George, *J. Am. Chem. Soc.*, 2017, **139**, 16568-16575.
33. M. Kumar, P. Brocorens, C. Tonnelé, D. Beljonne, M. Surin and S. J. George, *Nat. Commun.*, 2014, **5**, 5793.
34. A. Mishra, S. Dhiman and S. J. George, *Angew. Chem. Int. Ed.*, 2021, **133**, 2772-2788.
35. J. Deng and A. Walther, *Adv. Mater.*, 2020, **32**, 2002629.
36. N. Mackman, *Nature*, 2008, **451**, 914-918.
37. X. Fu, L. Chen and J. Li, *Analyst*, 2012, **137**, 3653-3658.
38. G. H. Aryal, G. R. Rana, F. Guo, K. W. Hunter and L. Huang, *Chem. comm.*, 2020, **56**, 13437-13440.
39. S. M. Bromfield, E. Wilde and D. K. Smith, *Chem. Soc. Rev.*, 2013, **42**, 9184-9195.

View Article Online
DOI: 10.1039/D4TB00862F

40. A. C. Rodrigo, S. M. Bromfield, E. Laurini, P. Posocco, S. Pricl and D. K. Smith, *Chem. comm.*, 2017, **53**, 6335-6338.
41. F. Zsila, T. n. Juhász, G. Kohut and T. s. Beke-Somfai, *J. Phys. Chem. B*, 2018, **122**, 1781-1791.
42. H. Lee, B. In, P. K. Mehta, M. Y. Kishore and K.-H. Lee, *ACS Appl. Mater. Interfaces*, 2018, **10**, 2282-2290.
43. M. Halat, G. Zając, V. Andrushchenko, P. Bouř, R. Baranski, K. Pajor and M. Baranska, *Angew. Chem. Int. Ed.*, 2024, e202402449.
44. N. H. Mudliar, P. M. Dongre and P. K. Singh, *Sens. Actuators, B*, 2019, **301**, 127089.
45. S. Kotha, M. F. Mabesoone, D. Srideep, R. Sahu, S. K. Reddy and K. V. Rao, *Angew. Chem. Int. Ed.*, 2021, **133**, 5519-5526.
46. K. V. Rao and S. J. George, *Chem. Eur. J.*, 2012, **18**, 14286-14291.
47. B. Wang and C. Yu, *Angew. Chem. Int. Ed.*, 2010, **8**, 1527-1530.
48. Z. Chen, V. Stepanenko, V. Dehm, P. Prins, L. D. Siebbeles, J. Seibt, P. Marquetand, V. Engel and F. Würthner, *Chem. Eur. J.*, 2007, **13**, 436-449.
49. S. Kang, T. Kim, Y. Hong, F. Würthner and D. Kim, *J. Am. Chem. Soc.*, 2021, **143**, 9825-9833.
50. F. Fennel, J. Gershberg, M. Stolte and F. Würthner, *Phys. Chem. Chem. Phys.*, 2018, **20**, 7612-7620.

UNIVERSITAT DE BARCELONA

View Article Online
DOI: 10.1039/D4TB00862F

16 June 2024

Dear Prof. Kaushik Chatterjee,

Associate Editor, Journal of Materials Chemistry B

Manuscript ID: TB-COM-04-2024-000862

The authors confirm that the data supporting the findings of this study are included within the manuscript and its supplementary material. Additionally, the raw data can be made available upon reasonable request.

Best regards,

Mohit Kumar, PhD

Assistant Professor
Department of Inorganic and Organic Chemistry
University of Barcelona
Barcelona, Spain-08028
Email: mohit.kumar@ub.edu
Ph: +34-934039090